Jurnal Teknologi

Full Paper

EMPIRICAL MODEL FOR WATER PENETRATION OF SEA WATER TO PREDICT CONCRETE COVER

Chatarina Niken*, Ratna Widyawati, Mohammad Isneini, I Gusti Komang Satria Guna Wibawa

Civil Engineering Department, Faculty of Engineering, University of Lampung, Sumantri Brojonegoro street No 1, 35141, Rajabasa, Bandar Lampung, Indonesia

Article history
Received
30 April 2025
Received in revised form
16 July 2025
Accepted
4 August 2025
Published Online
30 April 2026

*Corresponding author
maman@uxm.edu.my

Graphical abstract

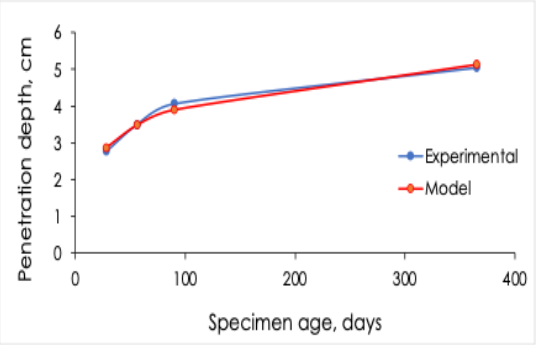

Abstract

Small docks play a vital role in supporting economic activities in Indonesia, where concrete is commonly used due to its perceived durability. However, exposure to seawater and wave action necessitates enhanced protection, as degradation of concrete in marine environments is ultimately unavoidable. This study examines seawater penetration into concrete at the Lempasing Fishermen's Boat Pier in Lampung Province, Indonesia, over a 365-day period. The research employed 22.5 MPa PCC concrete, which met the standard penetration depth requirements for highly aggressive environments. Samples were cured in freshwater for 7 days before exposure to seawater. The findings show that penetration depth conforms to the empirical model y = a ln(bt) + c, aligning with existing literature (Yoo *et al.*, 2011). Model projections estimate seawater penetration to reach approximately 8.5 cm over 50 years. Accordingly, a 13 cm concrete cover can serve as a sacrificial layer, effectively delaying the initiation of rebar corrosion and preserving reinforcement integrity for up to 50 years, with a safety factor greater than 1.5. Despite this protective strategy, the compressive strength of submerged concrete declined significantly to 7 MPa after 365 days. This deterioration was primarily due to continuous wave action and the chemical ingress of seawater, which triggered the formation of ettringite and pore expansion, resulting in cracking. Furthermore, the premature exposure of concrete—before achieving pore discontinuity—significantly contributed to the loss of strength. These findings underscore that while rebar corrosion can be mitigated through adequate cover, the concrete matrix itself remains vulnerable to accelerated internal degradation under aggressive marine conditions.

Keywords: Concrete, concrete cover, compressive strength, seawater penetration

1.0 INTRODUCTION

1.1 Problem Statement

Indonesia is an archipelagic nation consisting of approximately 17,380 islands, of which around 8,000 are inhabited. As a result, numerous small piers are needed to support local transportation, especially for fishing activities. Concrete is the material of choice for constructing pier structures due to its perceived durability—defined as the ability of a material to maintain its performance over time when exposed to environmental conditions—especially when compared to steel or wood. However, cases of failure have been observed in small piers. Figure 1a shows a collapsed pier, while Figure 1b depicts a pier that exhibited visible degradation just two years after construction. Seawater contains a high concentration of sulfates and salts, and the surrounding marine air also carries these aggressive agents. Their infiltration into concrete can significantly accelerate material degradation, compromising the structural integrity of the pier. The failure of these structures not only poses safety risks but also results in substantial economic losses. Most small piers are constructed using normal concrete without additional protection or durability enhancements. This raises a critical question: How can normal concrete be resistant to the marine environment?

(a)

(b)

Figure 1 Small piers in Indonesia: (a) Collapsed pier, (b) Degraded piers

1.2 Mechanisms of Water Ingress

Durability in marine environments refers to a material's capacity to withstand continuous exposure to harsh environmental conditions. Concrete is commonly selected for pier structures due to its inherent durability, which refers to a material's ability to maintain its performance over time when subjected to environmental stressors. However, achieving optimal durability requires appropriate design, quality construction, and ongoing maintenance [1]. A high level of concrete durability can only be attained when both the material's properties—at macro and micro scales—and environmental influences are thoroughly understood. Concrete is a porous material, with a total pore surface area reaching approximately 500 m^2/cm^3[2]. The diameter of these pores ranges between 10 nm and 1000 nm, which is large enough to allow the passage of water molecules that typically measure around 3 Å (0.3 nm). Through these pores, water can transport particles with diameters ranging from 10 nm to 700 nm (0.00001 mm to 0.0007 mm). As noted by Hand *et al*. (2019) [3], the penetration of water into concrete is influenced by pore radius and the size of the transported particles. Open and interconnected pores form capillary pathways that facilitate water ingress, which may occur via pressure gradients, diffusion, or capillary action.

Sources of water ingress include rainfall, soil moisture, humidity in the surrounding air, wave splashing, and capillary rise. The continuity of pores plays a significant role in determining the speed at which harmful substances such as sulfates and chlorides reach embedded reinforcement. Once inside the concrete, water can raise internal humidity, initiate further hydration reactions with unhydrated cement particles, dissolve hydration products, alter the internal pH, and further modify the pore structure. In splash zones, where both moisture and oxygen are abundant, corrosion may be limited, but degradation of the concrete matrix progresses more rapidly due to repeated wetting and drying cycles and chemical attack [4].

The effects of water ingress into concrete include strength reduction, cracking, increased permeability, and corrosion of embedded steel. Therefore, the concrete used in pier structures must not only prevent water infiltration but also resist the aggressive substances dissolved in seawater that accelerate degradation. The concrete cover serves as a crucial protective layer, and its durability depends on adequate thickness and material resistance. Achieving resistance requires minimizing both porosity and permeability, thus enhancing the concrete's ability to function effectively throughout its intended service life.

1.3 Concrete Properties Affecting Permeability

Permeability in cementitious materials is a critical indicator of durability, as it determines the extent to which water and aggressive agents can infiltrate the concrete matrix. Low permeability signifies that the concrete is watertight and resistant to fluid ingress. Both low porosity and low permeability are essential characteristics of durable concrete [5]. Several factors, including the type and composition of materials, curing methods, exposure age, and environmental conditions influence these properties. Permeability decreases with an increase in pore discontinuities. The formation of discontinuous pores is delayed by higher water-to-cement (w/c) ratios, as they require more extended periods to develop [6]. Pore discontinuities help reduce capillary porosity, which, along with surface cracks, is a principal contributor to increased permeability [7]. The incorporation of calcined clay has been shown to reduce macropores and promote the development of denser calcium-alumino-silicate-hydrate (C-A-S-H) and monosulfate (AFm) phases, thereby enhancing impermeability [8]. Research suggests that an optimal w/c ratio of approximately 0.28 results in minimal void permeability [9]. Similarly, the water-to-binder (w/b) ratio plays a pivotal role in hydration dynamics; lower w/b ratios combined with extended curing periods improve resistance to water diffusion [10]. In contrast, higher w/c ratios and insufficient curing result in reduced compressive strength and increased permeability [6].

Among supplementary cementitious materials, silica fume has demonstrated superior performance in enhancing water tightness compared to plain concrete and concrete containing crystalline additives, particularly under moisture-limited conditions [7]. A synergistic combination of 9% micro-silica (SiO_2) and 1% nano-silica reduced water penetration in self-compacting concrete (SCC) by nearly 58%, short-term water absorption by approximately 23%, and total absorption by about 30% [11]. Furthermore, the use of modern polycarboxylate ether-based superplasticizers and chemically active additives significantly improves permeability control, compressive strength, and overall concrete performance [12]. Nevertheless, permeability tends to increase with higher proportions of recycled aggregates due to their inherent porosity [13]. On the other hand, encased concrete structures show a marked reduction in penetration depth with the addition of multiple carbon fiber-reinforced polymer (CFRP) layers, enhancing impermeability [14].

Water penetration in concrete can also be driven by external pressure. Water tightness, therefore, becomes a decisive factor in evaluating a structure's ability to resist pressurized fluid ingress [15]. Experimental studies have been conducted to assess penetration depth under forced water pressure conditions [16]. Fly ash has proven effective in reducing water penetration depth under pressure by increasing concrete density and enhancing watertight properties [17]. This finding aligns with the conclusions drawn by Hearn *et al*. (2006) regarding SCC [6] However, the benefits of fly ash in improving durability under seawater exposure are notably limited when its content exceeds 10% [18].

1.4 Existing Research and Standards

Concrete undergoes continuous changes over time due to chemical exposure, water infiltration, material composition, environmental conditions (such as heat and humidity), and sustained mechanical loads. These factors contribute to the evolution or degradation of the concrete matrix by altering its pore structure, chemical composition, and mechanical integrity. As such, concrete porosity is a complex and dynamic property rather than a static characteristic. The development of pore structure is governed not only by the initial hydration process but also by subsequent degradation mechanisms induced by environmental exposure [6].

According to the Japanese Specification on Concrete Standard (2017), water penetration must be evaluated to control the risk of reinforcement corrosion caused by chloride ingress from seawater [5]. Chloride-induced corrosion is a major cause of structural degradation in marine environments. A study investigating the combined effects of fatigue loading and hydrodynamic pressure on chloride penetration in road pavements revealed that stress levels significantly influence the chloride ion diffusion coefficient (DRCM), particularly when the number of load cycles ranges between 30,000 and 60,000. Additionally, hydrodynamic pressure was shown to accelerate damage accumulation and influence DRCM behavior during the final loading stages [19].

For sulfate exposure classifications, categories S0 (no exposure), S1 (slight exposure), S2, and S3 are determined based on the concentration of sulfate ions (SO_4^{2-}). Seawater is classified under the S1 category, where the maximum allowable SO_4^{2-} concentration is 1500 ppm [20]. In addition, [21] recommends that the chloride ion content in concrete should not exceed 0.5 g/L (0.05%) to ensure long-term durability, particularly in structures exposed to marine environments.

1.5 Knowledge Gap

To prevent chloride ions from reaching the reinforcement, waterproof concrete and a sufficiently thick cover are required, especially in marine environments where seawater contains aggressive substances and is subjected to continuous wave pressure. However, Indonesian standards do not specify a concrete cover thickness for such conditions. The largest concrete cover requirement in Indonesia applies to underground structures, with a minimum thickness of 7.5 cm [20]. Waterproof concrete is defined as concrete with a maximum penetration depth of 50 mm for moderately

aggressive environments and 30 mm for highly aggressive environments [22]. Additionally, it must have a maximum permeability coefficient of 1.5 × 10^{-11} m/dt, as specified in [ACI 301-729] [23].

1.6 Objectives of This Study

No matter how dense, concrete always contains several interconnected pores, making it an inherently permeable material. Some permeability testing methods pose challenges in terms of time, cost, and variability. Therefore, improved rapid permeability testing is needed to enable agencies to adopt performance-based specifications with greater confidence [24]. Recent predictive approaches, including Ensemble and Regression Tree (RT) models, have demonstrated high accuracy in estimating water penetration depth [25].

Although predictive models exist, further studies are required to assess the actual conditions at pier locations. These models can provide insights into the necessary concrete cover thickness. In marine construction, the concrete cover must account for degradation depth, ensuring that the inner structure remains strong enough to withstand applied loads over its service life. The growth of degradation depth in actual conditions and the relationship with the results of permeability tests according to standards are the objectives of this study. Thus, this study can help predict the degradation of concrete submerged in seawater based on these tests.

2.0 METHODOLOGY

The research was carried out experimentally, using a concrete mix designed to achieve a target compressive strength of 20.75 MPa. The mixture composition for 1 m³ of concrete is presented in Table 1.

Table 1. Material Composition for 1 m³ of Concrete

No	Materials	Amount (kg)
1	PPC	379.63
2	Water	205
3	Coarse aggregate	1013.75
4	Fine aggregate	741.01

This study utilizes Portland Pozzolan Cement (PPC) due to its availability in remote areas, where Ordinary Portland Cement (OPC) is scarce. Additionally, PPC contributes to reducing global warming impacts.

Selection w/c 0.54

The water-to-cement ratio of this mixture is 0.54. Qu *et al*, 2021 [26], published a critical review of 11 studies on the durability deterioration of concrete in marine environments, covering both materials and structures. Among the reviewed papers, nine were conducted in real marine conditions, including the Gulf of Thailand, Arabian Gulf, Persian Gulf, Beibu Gulf, and Wheat Island. These studies used OPC and OPC combined with varying amounts of fly ash, GGBS, and silica fume. The water-to-binder (w/b) ratios ranged from 0.35 to 0.72.

Concrete used in the Persian Gulf, Beibu Gulf, and Wheat Island adopted a w/b ratio of 0.35, while studies in Thailand and other regions used ratios from 0.4 to 0.72. This study employs PPC, which includes fly ash, and therefore a w/b ratio of 0.54 was selected. This value closely resembles the w/b ratio used in the Gulf of Thailand study, which applied OPC with 15% fly ash and a w/b of 0.55 for structures aged 5 years. Additional studies reviewed by Qu *et al*. (2021) with similar w/b values include research in the Arabian Gulf (OPC, w/b 0.5) and in the tidal zone along the English coastline at Folkestone, UK (OPC + 30% PFA, w/b 0.56) [27].

Selection of Standard Penetration Test Methods

The measured penetration depth reflects the condition of field concrete under hydraulic pressure. This test has demonstrated good correlation between water penetration and surface resistivity.

Standard penetration tests were conducted at the Structure and Materials Laboratory of the University of Indonesia. Permeability testing was carried out on all sample types—three samples each—according to the Deutsches Institut für Normung (DIN) EN 12390-8: 2009-07 [28] . This standard requires that permeability be assessed in concrete aged 28 days. The test involves applying water pressure to concrete block specimens measuring 200 mm × 200 mm × 120 mm. The water pressure is applied incrementally: 1 bar (1 kg/cm²) for the first 48 hours, 3 bar for the next 24 hours, and 7 bar for a final 24 hours. After the pressure is applied, the specimen is split to determine the depth of water infiltration.

Compression tests and seawater penetration tests were conducted at 28, 56, 90, and 365 days using cylindrical specimens with a diameter of 15 cm and a height of 30 cm, in accordance with the Indonesian National Standard SNI 03-2491-2002 [29]. The seawater penetration test used specimens from split tensile testing, and the penetration depth was determined visually based on the depth of water infiltration indicated by visible color differences. All testing was performed at the Materials and Construction Laboratory, University of Lampung, Indonesia. Penetration depth was measured using vernier calipers at the deepest point of infiltration (Figure 4d).

Selection of Sample Shapes

Pier pillars are generally cylindrical, making cylindrical samples more representative of real structural conditions.

Treatment of Samples

After the concrete was poured into the mold, the surface was covered with plastic to prevent water loss. At one day of age, the mold was removed, and the concrete was soaked in a tub for seven days. Following the curing period, some specimens were stored in a protected environment, while others were placed in seawater at the Lempasing Fishing Boat Pier, Bandar Lampung, Indonesia. At 28, 56, 90, and 365 days, six specimens were retrieved from the sea at each interval—three for compressive strength tests and three for penetration tests. To maintain their condition, the test specimens were wrapped in aluminum foil and immediately transported to the Materials and Construction Laboratory, University of Lampung, for testing.

Data analysis

Compressive strength tests were also performed on the protected specimens. All test results were verified using the Dixon Criterion[30].

The relationship between penetration depth and concrete age was analyzed and transformed into a logarithmic model, following the approach of [31]. The model coefficients were determined through trial and error by selecting values that produced the smallest sum of squared errors [32]. The model was then validated using the research findings of [33]. Once established, the model was used to predict penetration depths for future years.

The selected mixture also showed a standard penetration depth below the maximum allowable value for highly aggressive environments, which is 30 mm. This threshold of 30 mm is applied and interpreted as follows: if the standard penetration is less than 30 mm, the mixture is considered suitable for use in highly aggressive environments [22]. Samples for both the standard and real penetration tests were cured by immersion in fresh water for seven days. After curing, samples for the standard penetration test were kept in a protected environment, while samples for real penetration were placed at the pier site at the age of 9 days. Concrete samples from the actual location were tested at specific ages—28, 56, 90, and 365 days. Thus, at the age of 28 days, two types of penetration values are available: standard and real penetration. Real penetration data at various ages display distinct behaviors. If penetration growth continues to increase, concrete degradation is ongoing; if the growth stagnates, it indicates that penetration has ceased or slowed significantly. The standard penetration value acts as a reference—whether degradation will persist or plateau at a given age.

For normal concrete, in which penetration continues to increase, the penetration thickness provides guidance for how much concrete must be "sacrificed" to protect the reinforcement until the target service life is reached. The durability of a column in marine conditions must consider the effective cross-sectional area of sound concrete, reduced by the depth of the degraded zone, according to the designed lifespan.

The depth of water penetration was identified visually, both in standard penetration tests and in split tests for natural penetration. The standard penetration test conducted at 28 days at the University of Indonesia can be compared with real penetration tests conducted at the University of Lampung. Comparing the two supports the objectivity of penetration depth observation. In both types of tests, penetration depth was measured from the outer edge of the sample to the center, using split specimens tested under a split tensile load. The research flow is illustrated in Figure 2.

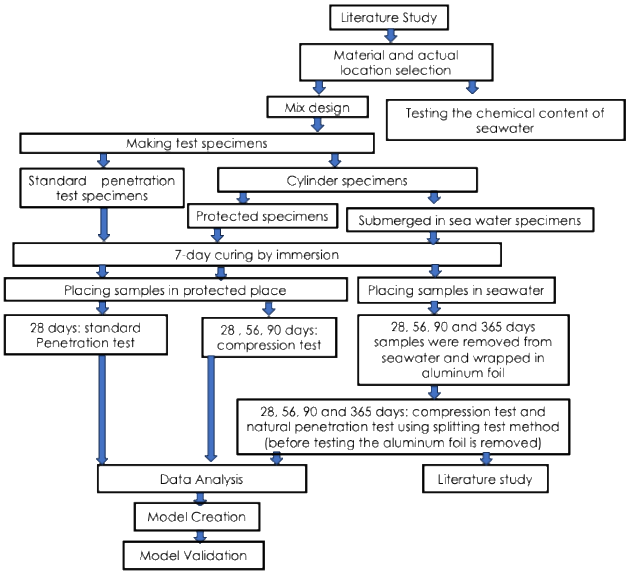

Figure 2 Research flow

3.0 RESULTS AND DISCUSSION

3.1 Results

Concrete samples submerged in seawater at the Lempasing Fishing Boat Pier, Lampung Province, Indonesia, were retrieved at 28, 56, 90, and 365 days (Figure 3).

Figure 3 Sampling from the seabed

The appearance of the samples at 28, 56, 90, and 365 days is shown in Figure 4.

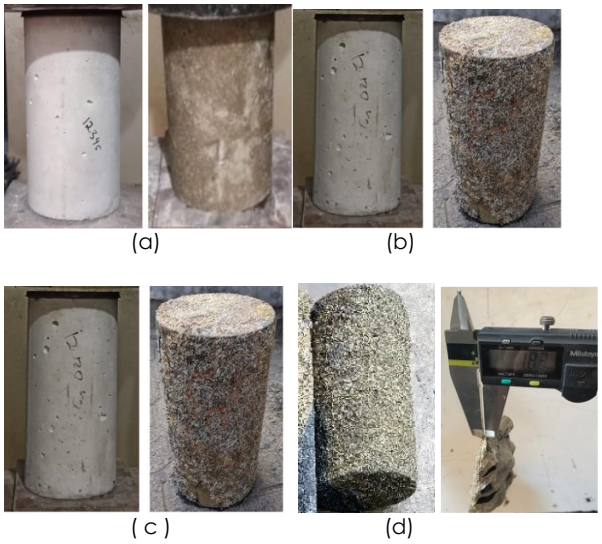

Figure 4 Compression test specimens: Protected specimens (left in a, b, and c) and seawater-immersed specimens (right in a, b, c, and d): (a) 28 days, (b) 56 days, (c) 90 days, (d) 365 days (submerged and cross-section of the concrete surface with macrofouling in dry condition)

The compressive strength of both protected and seawater-immersed concrete specimens is shown in Figure 5. Although the concrete used Portland Pozzolan Cement (PPC)—which undergoes a pozzolanic reaction that is not fully optimized at early ages—the target compressive strength of 20.75 MPa was achieved at 28 days (Figure 5).

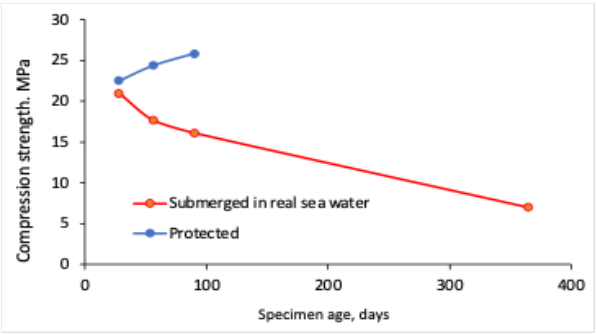

Figure 5 Compressive Strength of Protected and Seawater-Immersed Concrete

The test specimen after the standard penetration test is shown in Figure 6.

Figure 6 Sample section from standard permeability test

The results of the standard permeability test are presented in Table 2.

Table 2 Standard penetration test results

Maximum water penetration, mm					
Sample 1		Sample 2		Sample 3	
32.4	32.7	22.0	22.8	25.5	23.9

All test results in Table 2 were processed using the Dixon criteria in accordance with [30] at a 10% significance level (Figure 7). The standard deviation of the data shown in Table 2 is 2.5.

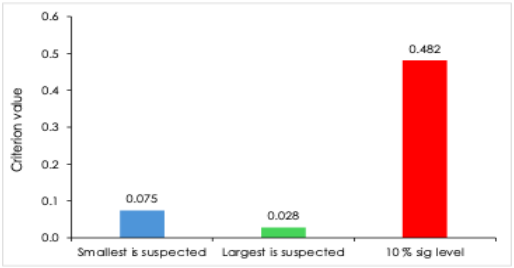

Figure 7 Standard penetration data acceptance check using Dixon criteria

Since all penetration test results (Table 2) fall within the 10% significance level threshold (Figure 7), all results are considered valid, and the average penetration depth was calculated. The average penetration depth is 26.55 mm, indicating that the concrete mixture meets the requirement for strongly aggressive environments, as it remains below the 30 mm threshold [22].

The empirical model is derived from experimental data. The selection of the logarithmic model is based on the following rationale: the penetration of sulfates and chlorides causes local imperfections in the concrete, leading to the appearance of lattice voids and subsequent diffusion. Atoms migrate across grain boundaries, resulting in convex or concave grain surfaces depending on the grain size. Grain size evolves over time, and minor impurity phases inhibit atomic particle growth. These impurity effects are

best represented using natural logarithmic functions [34].

The empirical model is presented in Equation 1:

$y = a \ln (bt) + c$ .....(1)

Where:

y : penetration depth (cm)
t : age (day/hour)
a : the influence of the permeability coefficient especially at 90-365 days – 0.88
b : the influence of the permeability coefficient especially at 56-90 days—0.8
c : the influence of the permeability coefficient especially at 28 days –0.1355

The coefficients were determined through trial and error, selected to minimize the sum of squared errors (SSE) and produce the model that best fits the experimental data. Regression diagnostics are shown in Figure 8.

The relationship between penetration depth and the empirical model is illustrated in Figure 8.

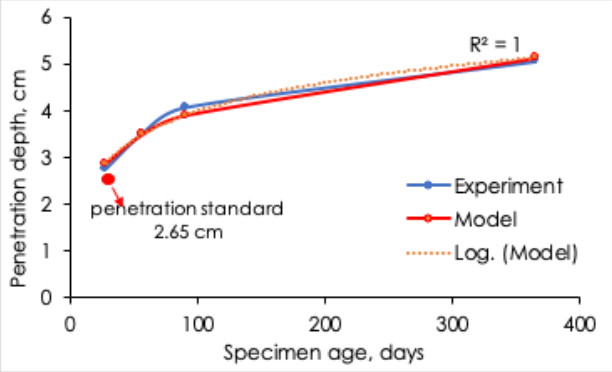

Figure 8 Comparison of experimental and model penetration depth

The sum of squared errors (SSE) [35] for the model was calculated as 0.046, which is less than 5%, and R^2 is 1 (Figure 8), indicating a high level of accuracy.

In real-world conditions, the most consistent factor is the chemical composition of seawater, which is reflected by the constant "c" in Equation 1. According to Darcy's Law, fluid flow is defined as:

$Q = -K.A\ \Delta H/\Delta L$

Where:
Q = the fluid flow rate
K = permeability coefficient
A = cross-sectional area penetrated by the fluid
Δh = difference in piezometric height between two points,
ΔL = distance between the two points.

Concrete exposed to seawater undergoes pore structure changes over time due to chemical interactions, making the permeability coefficient (K) in Equation 1 a time-dependent factor, expressed as a. The area (A in Darcy's law) affected by fluid flow also changes with time due to the development of atomic structure, which is represented as ln(bt) in the model. The natural logarithmic form was selected because minor impurity phases, which inhibit atomic particle growth, evolve over time—a behavior best captured logarithmically.

For validation, the model was applied to the study by Yoo *et al*. [33] (Figure 9) using coefficients: a = 1.704; b = 0.5; c = - 2.4138.

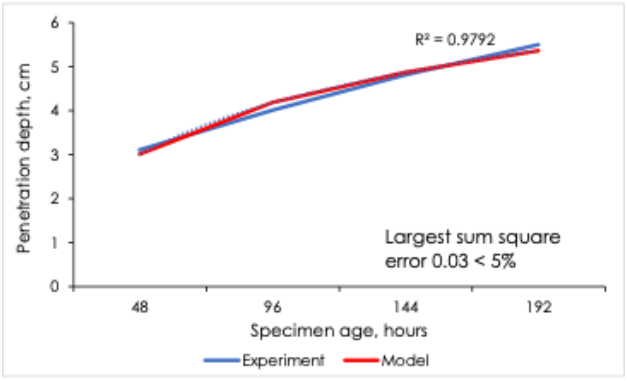

Figure 9 Application of the model in the research of Yoo *et al*, 2011

The error value when applying the model to Yoo *et al*.'s [33] results was 0.0669, using the sum of squared errors method [35]. Yoo *et al* [33] investigated penetration depth under water pressure conditions.

Using the model in Equation 1, the predicted seawater penetration depth into concrete over time is presented in Figure 10.

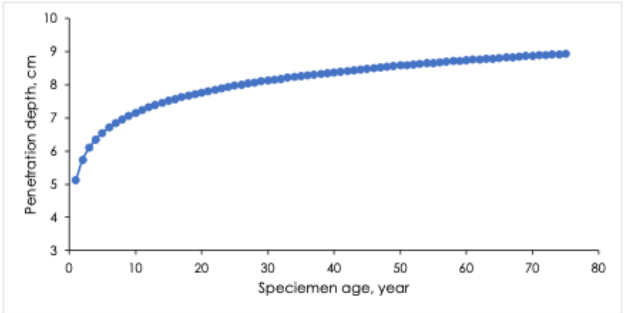

Figure 10 Prediction of seawater penetration depth into concrete

The conversion of the water-to-cement (w/c) ratio to penetration depth and estimated service life based on capillary pores is presented using Zheng *et al*.'s research [36] in Formula 2, and its implementation scenario is summarized in Table 3.

Where:

C_t: cover for t years with selected w/c; C_{model}: concrete cover model at age t; $Cap_{p\text{-}submerged}$: Capillary pores when concrete comes into contact with seawater; $Cap_{p\text{-}submerged\text{-}model}$: capillary pores model.

Table 3 Implementation scenario

w/c	Standard penetration, cm	Capillary pores, % dry mass at .. days of age		Concrete cover, cm			
				Concrete in contact with the sea, …. days of age			
	28	14	28	14	28	14	28
				50 years		75 years	
0.44	2.08	19.9	18	6.49	5.88	6.8	9.3
0.50	2.42	22.9	21	7.47	6.87	7.8	10.8
0.54	2.66	24.9	23	8.13	7.52	8.6	11.8

he required concrete cover thickness to reach service lives of 50 years and 75 years, based on the empirical model shown in Figure 10, is 8.5 cm and 8.9 cm, respectively. From Table 3, the cover thickness calculated for a w/c of 0.54 is 8.13 cm for 50 years and 8.6 cm for 75 years, showing consistency with the model predictions.

To ensure structural safety, a safety factor of 1.5 is applied. The resulting recommended cover thickness is presented in Table 4.

Table 4 Implementation criteria with safety factor 1.5

w/c	Concrete cover with safety factor 1.5, cm			
	Concrete in contact with the sea, …. days of age			
	Service life 50 years		Service life 75 years	
	14 days	28 days	14 days	28 days
0.44	9.8	8.8	10.2	9.3
0.5	11.2	10.3	11.8	10.8
0.54	12.2	11.3	12.8	11.8

3.2 Discussion

The surface of concrete submerged in seawater gradually becomes covered with macrofouling and appears increasingly fragile over time (Figure 2). Marine organisms typically prefer concrete surfaces when the pH is neutral to slightly alkaline (i.e., higher pH values), rather than acidic (lower pH). However, macrofouling remains superficial, forming a layer approximately ±1.8 mm thick, as measured using a vernier caliper (Figure 4d, taken after drying), without penetrating the concrete. The concrete in this study meets the design strength requirement, achieving a compressive strength of 22.5 MPa (Figure 5), and also satisfies the penetration resistance criteria for strongly aggressive environments (Figure 6, Table 2, and Figure 8). Although Portland Pozzolan Cement (PPC) was used—which contains pozzolanic materials—the optimal pozzolanic reaction typically occurs around 56 days. All standard penetration test data in Table 2 were validated using Dixon's criteria (Figure 7), confirming their reliability.

3.2.1 Concrete Compressive Strength

The compressive strength of the concrete decreased gradually over time (Figure 5), declining to 7 MPa at 365 days. This significant reduction is primarily attributed to the chemical composition of the seawater at the study site, as detailed in Table 5.

Table 5 Chemical composition of seawater in Lempasing, Lampung, Indonesia

Chemical	mg/l	%
Cl	18859.4	56.6
Sulfate	2690.5	8.1
Na	10532.6	31.6
Mg	941	2.8
Fe	0.46	0
Ca	285.08	0.9
Cr	0.083	0
Al	0.11	0
P	0.362	0
Salinity	32 ppt	
pH	8.51	
Dissolved oxygen		
- dry season	5.5-7.2	
- rainy season	5.1-6.7	

This composition closely aligns with the findings of Galvis-Sánchez, which reported chloride (55.2%), sodium (30.6%), sulfate (7.7%), magnesium (3.7%), calcium (1.2%), potassium (1.1%), and trace amounts of other elements [37].

Concrete Temperature

The temperature within the concrete was measured using a vibrating wire embedded strain gauge installed in a 150 mm × 150 mm × 100 mm concrete column immersed in seawater along with the other research samples. The temperature trend recorded over time is shown in Figure 11.

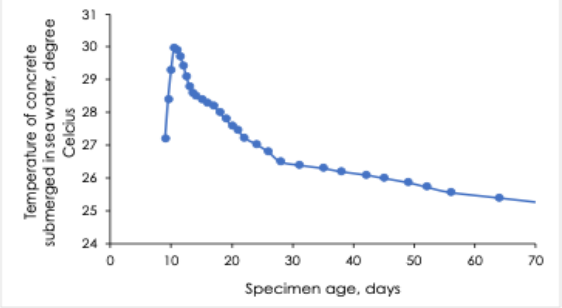

Figure 11 Temperature in concrete

Chloride Penetration

Tong *et al* 2025 [38], published findings on chloride penetration in cement paste with a water-to-cement ratio (w/c) of 0.6. The sample used had a diameter of 10 cm and a length of 50 mm, coated with silicon gel, and soaked in a 0.5 mol/L NaCl solution for 100 days. The specimens were maintained at two temperatures: 23°C and 38°C. Their results showed that higher temperatures in the paste led to more gradual chloride penetration at the same penetration depth. In Indonesia, the temperature of concrete is influenced by the ambient climate, averaging around 30°C (as shown in Figure 11). Based on chloride penetration data at 23°C and 38°C, a projected chloride penetration curve for 30°C was developed, illustrated in Figure 12.

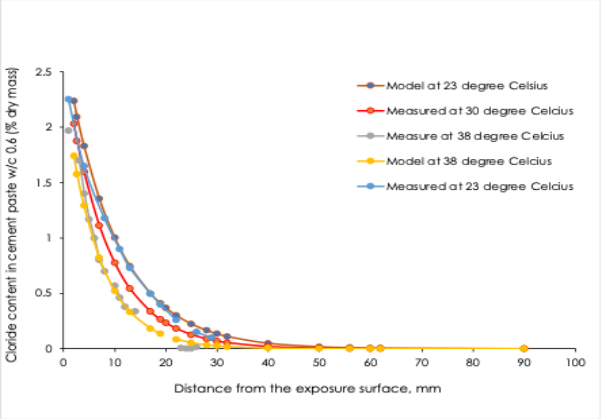

Figure 12 Chloride content in cement paste (Tong *et al*, 2025 [38] & Niken for Indonesia, red curve)

Capillary Pore

Zheng *et al*, 2021 [36] examined capillary pore content in cement paste with w/c ratios of 0.4, 0.44, and 0.5 at ages of 1, 3, 7, and 28 days. From this dataset, the capillary pore content for a w/c of 0.54 was extrapolated.

The concrete cover value at 50 years, derived from the empirical model in Figure 10, was found to be 8.5 cm. Meanwhile, using capillary pore analysis and chloride penetration estimations, the cover value was determined to be 8.13 cm (as shown in Table 3). This value exceeds the 60 mm threshold, beyond which chloride content is generally undetected (Figure 12). In real-world conditions, however, several factors differ significantly from controlled laboratory setups: varying chloride concentrations, differences between paste and concrete composition, lack of protective coatings, and wave-induced pressure on concrete structures. Therefore, the expected penetration depth in practice is assumed to be 1.5 times greater than that reported in the study by Tong *et al*. (2025) [38].

The standard penetration values for w/c ratios of 0.44 and 0.5 were calculated based on the corresponding capillary pore contents and are presented in Table 3. These values serve as the foundation for the implementation scenarios described in Tables 3 and 4.

pH

Seawater at the research location contains 2,690.4 mg/L of sulfate (Table 5), which falls into Exposure Class S2, as SO_4^{2-} levels are between 1,500–10,000 ppm [20]. The presence of sulfate (SO_4^{2-}) increases internal alkalinity (pH), and changes the hydration processThe presence of sulfate (SO_4^{2-}) increases the internal alkalinity (pH) and influences the hydration process [32]. The initial pH of concrete is typically around 12.5–13.5 due to the presence of calcium hydroxide. At pH > 10.5, sulfate reacts with aluminate phases and forms ettringite [39].

Sulfate and Chloride

Sulfate in seawater triggers the formation of secondary ettringite. The ratio of ettringite length to diameter decreases when chloride (Cl^-) enters the concrete, which induces expansion. This expansion weakens bond strength and leads to cracking. According to SNI 2847 [20], the maximum allowable chloride content from seawater is 0.15% by weight of cement. In this study, the chloride concentration in seawater was 18,859.4 mg/L. Given the PPC weight of 379.63 kg, the allowable chloride limit is 570 mg/L—meaning the Cl^- content at the site far exceeds the permissible threshold.

Chloride readily reacts with C_3A to form Friedel's salt. This direct formation leads to the accumulation of Al^{3+} in solution, released during the reaction of C_3A, along with Ca^{2+}. The presence of Ca^{2+} contributes to concrete expansion. The Friedel's salt structure also promotes the formation of tobermorite and ettringite ($3CaO \cdot Al_2O_3 \cdot 3CaSO_4 \cdot 32H_2O$), while simultaneously inhibiting portlandite ($Ca(OH)_2$) and calcium silicates ($2CaO \cdot SiO_2$ and $3CaO \cdot SiO_2$), especially in high-performance concrete (HPC) exposed to seawater between 3–90 days [40].

Tobermorite helps retain concrete strength, whereas ettringite is expansive, compounding the swelling effect induced by Ca^{2+}. This expansion may help narrow capillary pores, but if the expansion exceeds the pore volume, the resulting pressure can fracture the concrete matrix.

The formation of Friedel's salts via an ion-exchange mechanism involves the release of OH^- ions from AFm hydrates into the pore solution, which further raises the pH [41]. This adds to the pH increase already caused by sulfate ions. A higher pH causes morphological changes in AFt (ettringite), shifting from rod-like to needle-like forms, and reduces the formation of AH_3 gel. This transformation is accompanied by a rise in continuously connected pores and a decline in disconnected pores, ultimately resulting in weakened matrix strength [42].

Magnesium

The magnesium (Mg) content in seawater at the study site was 941 mg/L. Dissolved oxygen levels in the Lampung, Indonesia sea ranged from 5.1–7.2 mg/L (Table 5). This oxygen combines with Mg to form magnesium oxide (MgO), which can react with silica fume to form magnesium silicate hydrate (M-S-H). M-S-H gel is produced through the reaction between MgO and silica fume, forming a shell-like structure with internal cavities [43]. Magnesium also reacts with sulfate to produce magnesium sulfate, which is known to degrade concrete by decomposing calcium silicate hydrate (C-S-H) into M-S-H gel, leading to long-term deterioration.

In addition to forming oxides, Mg can combine with chloride (Cl^-) to form magnesium chloride ($MgCl_2$). While MgO has been considered as a component in cement due to its benefits such as high strength and dimensional stability, the high concentration of chloride at the research location (Table 5) makes the formation of $MgCl_2$ more likely. However, $MgCl_2$ can be detrimental to concrete, contributing to surface flaking and crumbling. Water containing Mg ions can diffuse into the silicate gel matrix of the concrete and bind calcium from the surface layer. This calcium loss destabilizes the C-S-H structure [39]. Additionally, the newly released magnesium can precipitate as brucite ($Mg(OH)_2$) within the concrete paste. Brucite crystal growth can generate internal stresses. It is known that the growth of gypsum and halite crystals can exert pressures exceeding 2000 atm (202.6 MPa), suggesting that similar stress levels may be possible with brucite. Such internal pressure leads to swelling and eventual failure of the concrete matrix [44].

Chromium and Iron (Ferro)

Chromium (Cr) and iron (Fe) are also present in seawater. When Cr is combined with Fe in slag, it can be used to replace up to 40% of sand in concrete mixtures, yielding improved compressive strength [45]. However, when Fe combines with oxygen, it oxidizes and causes corrosion of steel reinforcement.

Sodium in concrete is typically in the form of sodium chloride (NaCl), a salt that significantly degrades the durability and performance of concrete over time.

Phosphorus

In addition to the elements mentioned above, seawater also contains phosphorus. According to Liu *et al*. (2024) [46], increasing the amount of phosphorus waste in concrete can improve workability, but it tends to reduce the mechanical properties of the concrete.

Salinity

Although the salinity at the research site is below 500 ppm—technically making the seawater usable in concrete mixtures—the presence of harmful elements such as chloride, sulfate, and magnesium poses risks. Therefore, achieving optimal pore discontinuity and ensuring low permeability are crucial in marine concrete applications. The outer concrete layer (blanket) can act as a sacrificial barrier, protecting the core structural concrete from degradation.

Permeability

Intrinsic permeability and compressive strength both improve when the concrete matrix is denser and more compact. However, even small defects in the matrix—while negligible in their effect on compressive strength—can increase permeability by more than tenfold [47]. Therefore, compressive strength alone is not a reliable indicator for estimating the intrinsic permeability of concrete [6].

The maximum permeability coefficient for watertight concrete is 1.5×10^{-11} m/s, as specified by [ACI 301-729 (revised 1975)] in [23]. To achieve this level of impermeability, the penetration depth between 28–90 days must be approximately 8×10^{-7} cm. When translated into standard penetration test conditions as defined by [28] —where water is applied under a pressure of 5.09 ± 0.5 kg/cm² for 72 hours—the required penetration depth to maintain a permeability coefficient of 1.5×10^{-11} m/s becomes 3.9×10^{-6} cm.

Such low permeability can be achieved by implementing the following strategies: (1) Using fine-grained aggregates such as limestone, fine marble, or dense trap rock, paired with optimal w/c ratios of 0.66, 0.48, and 0.38, respectively [6].(2) Incorporating nanoparticles (e.g., silica fume) to refine the microstructure. (3) Enhancing pore discontinuity, which limits the pathways for water ingress.

The time required for a concrete mixture to develop a discontinuous pore structure is shown in Table 6.

Pore Discontinuity

An increased water-to-cement (w/c) ratio leads to a rise in capillary porosity (Table 6). Capillary pores are typically considered the remnants of the originally water-filled spaces in fresh concrete. As the w/c ratio increases—from 0.40 to 0.44 and then to 0.50—the volume of initial mixing water increases by 2.34% and 3.09%, respectively [36]. As a result, pore spacing and continuity increase, while pore discontinuity decreases, making the concrete more permeable.

Table 6 Time required to achieve pore discontinuity

Time required to achieve a discontinuous pore structure		
w/c	**Time required**	**Approximate degree of hydration required**
0.4	3 days	0.5
0.45	7 days	0.6
0.5	14 days	0.7
0.6	6 months	0.95
0.7	1 year	1
>0.7	impossible	>1

Source: Hearn *et al*, 2006 [6]

With wider spacing and increased capillary pores, it becomes easier for seawater to penetrate deeper into the concrete, thereby increasing its permeability. The pore structure with a high degree of discontinuity significantly affects the intrinsic permeability of concrete. Meanwhile, the free water content in hardened concrete is influenced by the water-to-cement (w/c) ratio, which in turn alters the effective permeability of the concrete [6]. The sensitivity of w/c to concrete permeability is illustrated in Figure 1 [9].

From Figure 13, it can be concluded that changes in w/c from 0.25 to 0.28 do not cause a rapid increase in permeability—indicating that the concrete is less sensitive to permeability in this range (a 0.01 increase in w/c causes only a 0.23 mm/sec increase in the permeability coefficient). However, the permeability increases rapidly when the w/c ratio changes from 0.28 to 0.31 (a 0.01 increase results in a 1.23 mm/sec increase in permeability). Under these conditions, the concrete becomes highly sensitive to permeability increases.

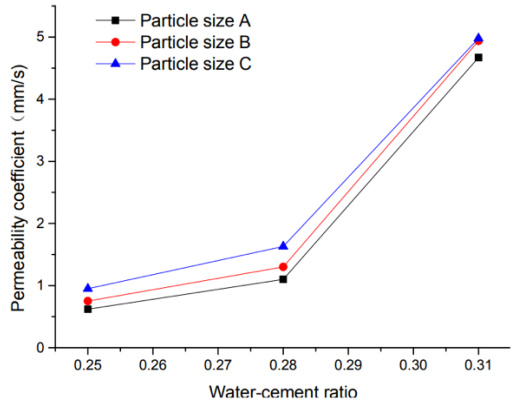

Figure 13 Relationship between w/c and concrete permeability

Although there is a direct correlation between concrete compressive strength and porosity [48], there is no direct relationship between porosity and permeability [31].

In addition to its impact on pore discontinuity, the w/c ratio also affects the compressive strength of concrete. Both the water-to-cement ratio and the curing method influence compressive strength to some extent. Even small changes in these parameters significantly affect the intrinsic permeability of concrete. Higher w/c ratios lead to a coarser pore structure and increased porosity.

Concrete structures in marine environments are continuously exposed to wave action, subjecting them to constant physical stress. This persistent pressure forces particles carried by seawater into the concrete, weakening its microstructure and increasing brittleness. Continuous wave action causes surface abrasion, leading to the detachment of loosely bound or microcracked particles. This results in gradual mass loss and a noticeable reduction in concrete strength.

Another contributing factor is the early exposure of concrete to seawater. In this study, the concrete was submerged at 9 days old, while pore discontinuity development was still incomplete at a w/c ratio of 0.54. According to [6], it is preferable to immerse concrete in seawater after 14 days, when the pore structure has had more time to become discontinuous and resistant to fluid ingress.

3.2.2 Experimental Model

Concrete immersed in seawater has a high degree of saturation. As saturation increases, effective permeability decreases, since the existing moisture clogs the pores. Therefore, water content significantly influences permeability [49]. The free water in hardened concrete affects effective permeability, whereas intrinsic permeability depends solely on the pore structure. A linear relationship exists between the log-transformed effective permeability and the degree of saturation, up to 70%. At high saturation levels, effective permeability correlates linearly with compressive strength. This relationship can be transformed into a natural logarithmic function. A comparison between the experimental model and observed results is presented in Figure 8, with an error of 0.046 and R^2 of 1.0, indicating excellent model accuracy. When water pressure is high, water flow within the concrete increases, resulting in seepage flow accompanied by internal deformation of the concrete[33]. Based on these findings, the experimental model follows Equation 1. An increase in the water-cement ratio (w/c) reduces the slope of this relationship, making effective permeability less sensitive to saturation variations [31].

The model was applied to the research findings of [33], which observed penetration under constant pressure for 8 days. Despite the limited duration, the model closely matched the data (Figure 9), with an error of 0.03 and R^2 of 0.9792. The slightly higher error is attributed to the constant-pressure conditions used in [33], whereas the present study used dynamically fluctuating pressure from real sea wave exposure.

The prediction of penetration depth up to 75 years was calculated using Equation 1 and is presented in Figure 10. At 50 years, the predicted penetration depth is approximately 8.5 cm, and at 75 years, it is 8.9 cm. The penetration rate begins to decline after 10 years, eventually stabilizing into a nearly linear trend. This shift occurs because seawater has saturated all pores, preventing further direct infiltration. From this stage forward, water movement within the concrete follows a seepage mechanism rather than pure penetration.

Applying a safety factor of 1.5, the recommended concrete cover is approximately 13 cm, which is advantageous for ensuring the structure remains durable beyond 50 years of service.

4.0 CONCLUSION

A study on the compressive strength and seawater penetration of concrete at the Lempasing Fishing Boat Dock, Lampung Province, Indonesia, has been conducted. The penetration results conform to the mathematical model: $y = a \ln(bt) + c$. This model has been validated against the research findings of [33] in Korea. Based on this model, the predicted penetration depths at 50 years and 75 years are approximately 8.5 cm and 8.9 cm, respectively. Therefore, constructing with a concrete cover of 13 cm is sufficient to ensure durability for 50 years, with a safety factor greater than 1.5.

The results indicate that concrete made with Portland Pozzolan Cement (PPC) and a w/c ratio of 0.54, when immersed in seawater at 9 days of age, experienced a significant drop in compressive strength, from 22.5 MPa to 7 MPa at 365 days. This reduction is primarily due to seawater penetration driven by wave pressure, which forces aggressive chemical particles into the concrete matrix. Additionally, reverse wave action may lead to chemical dissolution and further internal degradation. The early immersion of concrete, before optimal pore discontinuity was achieved, also contributed to the observed strength loss.

For improved durability, the use of PPC concrete with a w/c ratio of 0.5, and delayed exposure to the marine environment until at least 14 days of age, is considered appropriate. At this point, the concrete achieves optimal pore discontinuity, meaning the number of continuous pores is minimal. Seawater then enhances the pozzolanic reaction, promoting the formation of C-S-H and ettringite. The expansion of ettringite clogs the remaining limited pores, further preventing seawater ingress. This internal tightness, reinforced with a thicker concrete cover, ensures that the structure can achieve a service life of 50 years under marine conditions.

Acknowledgement

This research was fully supported by Mr. Heri Suhendi, the owner of the Lempasing Fishing Boat Dock in Lampung Province, Indonesia, to whom we express our sincere gratitude. We also extend our appreciation to the Laboratory of Materials and Construction, Faculty of Engineering, University of Lampung, for their assistance with testing. Additionally, we would like to thank Doni Irawan for his valuable support throughout the study.

Conflicts of Interest

The authors declare that there is no conflict of interest regarding the publication of this paper.

References

[1] Maraşlı, M., S. Subaşı, and D. Ramazanoğlu. 2023. Water Penetration Effects on Concrete Strength and Prevention Approaches. *Pioneer Contemporary Studies in Engineering*.

[2] Bazant, Z. P., and F. H. Wittmann. 1982. *Creep and Shrinkage in Concrete Structures*.

[3] Han, D., Z. Wang, Q. Wang, B. Wu, T. Yu, and D. Wang. 2019. Analysis of the Kozeny–Carman Model Based on Pore Networks. *Journal of Geophysics and Engineering*. https://doi.org/10.1093/jge/gxz089.

[4] Shi, J., Y. Zhao, and B. Zeng. 2020. Relationship between Pore Structure and Bending Strength of Concrete under High–Low Temperature Cycle Based on Grey System Theory. *Journal of Grey System*. 32(4).

[5] Kawano, M., and T. Kadano. 2024. Water Penetration Property of Concrete with Copper Slag Aggregate. *International Journal of GEOMATE*. 26(117).

[6] Hearn, N., R. D. Hooton, and M. R. Nokken. 2006. Pore Structure, Permeability, and Penetration Resistance Characteristics of Concrete. In *Permeability of Concrete*, edited by M. Alexander, S. Mindess, and J. Marchand. 77–92. London: Taylor & Francis.

[7] Cappellesso, V. G., N. dos S. Petry, M. A. Longhi, A. B. Masuero, and D. C. C. Dal Molin. 2022. Reduction of Concrete Permeability Using Admixtures or Surface Treatments. *Journal of Building Pathology and Rehabilitation*. 7(38).

[8] Liu, J., *et al*. 2022. Experimental Analysis on Water Penetration Resistance and Micro Properties of Concrete: Effect of Supplementary Cementitious Materials, Seawater, Sea-Sand and Water–Binder Ratio. *Journal of Building Engineering*. 50. https://doi.org/10.1016/j.jobe.2022.104153.

[9] Yang, H., R. Liu, Z. Zheng, H. Liu, Y. Gao, and Y. Liu. 2018. Experimental Study on Permeability of Concrete. *IOP Conference Series: Earth and Environmental Science*. 108. https://doi.org/10.1088/1755-1315/108/2/022067.

[10] Naderi, M., A. Kaboudan, and A. A. Sadighi. 2018. Comparative Study on Water Permeability of Concrete Using Cylindrical Chamber Method and British Standard and Its Relation with Compressive Strength. *Journal of Rehabilitation in Civil Engineering*.

[11] Almohammad-Albakkar, M., and K. Behfarnia. 2020. Water Penetration Resistance of Self-Compacting Concrete by Combined Addition of Micro and Nano Silica. *Asian Journal of Civil Engineering*. 22: 1–12.

[12] Skutnik, Z., M. Sobolewski, and E. Koda. 2020. Experimental Assessment of Water Permeability of Concrete with a Superplasticizer and Admixtures. *Materials*. 13(24). https://doi.org/10.3390/ma13245624.

[13] Koondhar, M. F., B. A. Memon, M. Oad, F. A. Chandio, and S. A. Chandio. 2020. Water Penetration of Concrete Made with Coarse Aggregates from Demolishing Waste. *Engineering, Technology & Applied Science Research*. 10(6): 6445–6449. https://doi.org/10.48084/etasr.3891.

[14] Amran, Y. H. M., R. Alyousef, H. Alabduljabbar, A. Alaskar, and F. Alrshoudi. 2020. Properties and Water Penetration of Structural Concrete Wrapped with CFRP. *Results in Engineering*. 5. https://doi.org/10.1016/j.rineng.2019.100094.

[15] Kozlica, S., E. Čehić, and S. Džidić. 2017. Experience in Testing of Concrete for Water Penetration during Construction of WWTP in Bihać. *Zbornik Radova Građevinskog Fakulteta*. 33(30): 433–440. https://doi.org/10.14415/konferencijaGFS2017.045.

[16] Yoo, J. Y., H. S. Lee, S. H. Tae, and M. B. Chul. 2007. Study on Water Penetration of Concrete under Water Pressure to Develop Anti-Corrosion Repair System. *Key Engineering Materials*. 348–349: 425–428. https://doi.org/10.4028/www.scientific.net/KEM.348-349.425.

[17] Adamus, J., and B. Langier. 2023. Analysis of Durability of Watertight Concretes Modified with Fly Ash. *Materials.* 16(17): 5742. https://doi.org/10.3390/ma16175742.
[18] Sudarsono, I., S. I. Wahyudi, and H. P. Adi. 2023. Fly Ash and Silica Fume Substitution on Compressive Strength and Permeability of Concrete in Marine Environment. *Jurnal Pensil Pendidikan Teknik*. 12: 281–292.
[19] Li, Y., A. Shen, S. Lyu, and Y. Guo. 2020. Chloride Ions Permeability of Pavement Concrete under Coupled Effect of Fatigue Loading and Hydrodynamic Pressure. *International Journal of Pavement Engineering.* 23(5): 1659–1674. https://doi.org/10.1080/10298436.2020.1819540.
[20] SNI 2847. 2019. *Persyaratan Beton Struktural untuk Bangunan Gedung*.
[21] Tjokrodimuljo, K. 2012. *Teknologi Beton*. 3rd ed. Yogyakarta: Biro Penerbit Teknik Sipil dan Lingkungan UGM.
[22] SNI 03-2914-1992. 1992. *Spesifikasi Beton Bertulang Kedap Air*.
[23] Neville, A. M., and J. J. Brooks. 1987. *Concrete Technology*. England: Longman Scientific & Technical.
[24] Milla, J., T. L. Cavalline, T. D. Rupnow, B. Melugiri-Shankaramurthy, G. Lomboy, and K. Wang. 2021. Methods of Test for Concrete Permeability: A Critical Review. *Advances in Civil Engineering Materials.* 10(1): 172–209. https://doi.org/10.1520/ACEM20200067.
[25] El-Mir, A., S. El-Zahab, D. Nasr, N. Semaan, J. Assaad, and H. El-Hassan. 2024. Machine Learning Models to Predict Water Penetration Depth in Concrete. *Journal of Building Engineering.* 95. https://doi.org/10.1016/j.jobe.2024.110107.
[26] Qu, F. 2021. "Durability Deterioration of Concrete under Marine Environment. *Journal of Building Engineering*.
[27] Bamforth, P. B., and W. F. Price. 1993. Factors Influencing Chloride Ingress into Marine Structures. Paper presented at *Economical Durable Construction through Excellence*, Dundee, UK.
[28] BSI 12390-8. 2009. *Testing Hardened Concrete – Depth of Penetration of Water under Pressure*. UK: Standards Policy and Strategy Committee.
[29] SNI 03-2491-2002. 2002. Metode Pengujian Kuat Tarik Belah Beton.
[30] ASTM E178-02. n.d. *Standard Practice for Dealing with Outlying Observations*.
[31] van der Merwe, J. E. 2022. "Estimation of Concrete Intrinsic Permeability. *Cement and Concrete Research.* 159: 106885. https://doi.org/10.1016/j.cemconres.2022.106885.
[32] Nainggolan, R., R. Perangin-angin, E. Simarmata, and A. F. Tarigan. 2019. K-Means Performance Using SSE and Elbow Method. *Journal of Physics: Conference Series.* 1361(1): 012015. https://doi.org/10.1088/1742-6596/1361/1/012015.
[33] Yoo, J. H., H. S. Lee, and M. A. Ismail. 2011. Water Penetration and Diffusion into Concrete under Pressure. *Construction and Building Materials.* 25(1): 99–108. https://doi.org/10.1016/j.conbuildmat.2010.06.052.
[34] Van Vlack, L. H. 1973. *A Textbook of Materials Technology*.
[35] Ardiansyah, Andi. n.d. Sum of Squared Errors (SSE) in Machine Learning. *Medium*.
[36] Zheng, S., *et al*. 2021. Effect of Water–Cement Ratio on Pore Structure Evolution. *Applied Sciences.* 11(7): 3063. https://doi.org/10.3390/app11073063.
[37] Galvis-Sánchez, A. C., J. A. Lopes, I. Delgadillo, and A. O. S. S. Rangel. 2013. Sea Salt. https://doi.org/10.1016/B978-0-444-59562-1.00026-8.
[38] Tong, L., B. Šavija, M. Zhang, Q. X. Xiong, and Q. Liu. 2025. Chloride Penetration under Environmental Variations. *Construction and Building Materials.* 458: 138380. https://doi.org/10.1016/j.conbuildmat.2024.138380.
[39] Lagerblad, B. 2001. Leaching Performance of Concrete from Old Structures.
[40] Bachtiar, E., *et al*. 2022. RETRACTED: Monitoring Chloride and Friedel's Salt in Concrete. *Case Studies in Construction Materials.* 17: e01208.
[41] Suryavanshi, A. K., J. D. Scantlebury, and S. B. Lyon. 1996. Friedel's Salt Formation Mechanism. *Cement and Concrete Research.* 26(5): 717–727.
[42] Guo, H., Y. Liu, B. Tai, Z. Zhang, and Y. Zhu. 2022. Effect of pH on Sulphoaluminate Cement. *Construction and Building Materials.* 325: 126848.
[43] Zhang, T., J. Zou, B. Wang, Z. Wu, Y. Jia, and C. R. Cheeseman. 2018. Magnesium Silicate Hydrate (MSH) Gel Characterization. *Materials.* 11(6): 909.
[44] Winkler, E. M., and P. C. Singer. 1972. Crystallization Pressure in Concrete. *Geological Society of America Bulletin.* 83(11): 3509–3514.
[45] Kopuri, M., N. A. G. K. Manikantakopuri, and K. Ramesh. 2019. Concrete with Ferro Chrome Slag.
[46] Liu, Y., L. Jiang, J. Li, Q. Zhang, L. Yang, and J. Cao. 2024. Concrete with Phosphorus Tailings. *Journal of Materials in Civil Engineering.* 36(9).
[47] Neves, R., F. Branco, and J. de Brito. 2012. Statistical Interpretation of Air Permeability. *Materials and Structures.* 45(4): 529–539.
[48] Abbas, A., M. Carcasses, and J. P. Ollivier. 2000. Gas Permeability vs Compressive Strength. *Magazine of Concrete Research.* 52(1): 1–6.
[49] Lee, J., and K. Harada. 2023. Permeability Estimation Based on Strength and Pore Size. *Journal of Asian Architecture and Building Engineering.* 22(1): 188–200.